X-RAY SCATTERING FROM RANDOMLY ORIENTED SUPERHELICES

CIRCULAR SUPERHELICAL DNA

CRAIG J. BENHAM, GEORGE W. BRADY, AND DAVID B. FEIN, *Division of Laboratories and Research, New York State Department of Health, Albany, New York 12201, and the Center for Biological Macromolecules, State University of New York at Albany, Albany, New York 12222*

ABSTRACT The scattering functions of randomly oriented filaments of finite length exhibiting two orders of helicity have been calculated. It is shown to a good approximation that each order scatters as if present alone as a first order helix of the same contour length and pitch angle. These results show that the measured scattering pattern from dissolved superhelical DNA molecules is consistent with the scattering pattern calculated for a coiled coil geometry.

INTRODUCTION

The double helical structure of DNA (Watson and Crick, 1953) was discovered a quarter of a century ago. More recently it has become apparent that other structural features involving the organization of many thousands of base pairs are also present in DNA molecules, at least when they are in closed circular form. These relatively tight conformations, called supercoils or superhelices, were postulated to explain the sedimentation velocity behavior of circular DNA (Bauer and Vinograd, 1968; Upholt et al., 1971; Gray et al., 1971). When intercalating agents such as ethidium bromide were added the sedimentation velocity first decreased to a minimum and then increased, consistent with the successive unwinding and rewinding of a helix of a higher order than that of the Watson-Crick helix. The existence of these supercoils is now known to have important biological consequences. It has been shown that the interactions of DNA with certain enzymes involved in transcription and replication events are strongly influenced by the state of supercoiling of the DNA (Wang, 1974). Certain enzymes. called topoisomerases, have been isolated from the nucleus which relax supercoils (Champou· and Dulbecco, 1972). Further, other enzymes called gyrases are found which introduce supercoils into relaxed DNA (Gellert et al., 1976). These two results together suggest some biological role for superhelicity. Again, supercoiled DNA has been shown to be the primary substrate involved in the integration of bacteriophage λ DNA into the chromosome of its host (Mizuuchi, Gellert, and Nash, 1978). It has also been suggested that superhelices enhance the probability of initiation of genetic recombination events (Holloman et al., 1975).

Supercoiling of closed circular DNA is conveniently discussed in terms of the linking number *Lk*, a fixed integer measuring the number of times either strand links through the

---

Dr. Benham's present address is the Department of Mathematics, University of Kentucky, Lexington, Kentucky 40506.

closed circle formed by the other strand. Lk cannot be varied unless one of the strands is cut, thus it is independent of the molecular shape so long as ring closure is preserved. This Lk may be decomposed into the sum of two terms (Fuller, 1971; Crick, 1976):

$$Lk = Tw + Wr. \tag{1}$$

Tw, the total twist, measures the number of times either strand twists around the central axis of the molecule. Wr, the writhing number, measures the bending of the central axis (Fuller, 1978). Both Tw and Wr may vary as the molecular shape changes, even though their sum, Lk, remains fixed. Thus the constraint imposed by ring closure consists of a coupling between bending and twisting.

Consider a linear DNA molecule all of whose Watson-Crick base pairs are hydrogen-bonded together so that it is neither overwound nor underwound. Let this molecule be closed into a ring by deforming it into a circle and bonding the ends. Such a closed circular molecule is said to be relaxed, with linking number Lk_0. An otherwise identical molecule may close with a different Lk, in which case it will be under stress and will deform from the unstressed equilibrium shape specified by Lk_0. Such a molecule is said to be supercoiled. The supercoiling is designated as either positive or negative depending on whether Lk is greater or less than Lk_0. We will assume in the following that the supercoiling is negative, since this holds true for many naturally occurring closed DNAs. From Eq. 1 it is evident that the stress, specified by the deficiency $\Delta Lk = Lk - Lk_0$, will be partitioned between Tw and Wr. The molecule will attempt to relieve the stress by twisting and/or bending. For a large stress, the deficiency in Tw may in turn be partitioned between local denaturation and a smooth decrease in the angular twist rate of the remaining double helical portions of the molecule. The relative amounts of smooth twisting, local denaturation, and bending which occur for a given value of Lk are those which minimize the total conformational free energy in the local environment. Local strand separation (melting) in superhelical DNA has been observed in the electron microscope (Brack, Bickle, and Yuan, 1975). Its presence has also been inferred from the chemical and physical behavior of supercoiled DNA (Lau and Gray, 1979; Wang, 1974; Dean and Lebowitz, 1971; Beerman and Lebowitz, 1973). Because the stiffness of single stranded DNA is small (Bloomfield, Crothers, and Tinoco, 1974), the flexibility at the sites of local melting permits the DNA to fold back on itself to form branched structures such as those observed by Campbell and Eason (1975) and Campbell (1976).

Despite the great interest in the supercoiling phenomenon, it has proved to be surprisingly difficult to determine the structural features of the superhelical conformation. To date the only direct experimental technique to be used successfully has been small angle diffraction (Brady et al., 1976). Although the measurements were hindered by the low scattering intensity and by the nicking effect of the incident radiation, which leads to a gradual fading out of the diffraction pattern during the course of the experiments, a preliminary Bragg's law analysis (in the absence of a more adequate theory) indicated that two orders of supercoiling appeared to be present. Two sets of peaks in the correlation ranges of ~340 and ~2,100 Å were observed. These disappeared when the samples were nicked (and thus unwound) by pancreatic DNase. They shifted towards smaller angle (large distance) on addition of ethidium bromide, disappeared at the ethidium bromide concentration corresponding to that where the minimum in the sedimentation velocity curve is observed, then reappeared again at

the higher ethidium bromide concentrations. Noncircular calf thymus DNA did not exhibit any of these effects. In other words, the observed diffraction effects behaved qualitatively as if they did arise from the type of superhelical structure postulated by Vinograd et al., only with two orders present.

Quite independently Benham (1977), in a theoretical analysis of the effects of forces applied to the ends of linear or to closed ring DNA molecules showed that the resulting equilibrium configurations were biperiodic, that is, exhibited two orders of supercoiling. The analysis was not developed to the point where quantitative shape predictions were possible, and thus no relation between the parameters (pitch, radius) of the two orders was derived; this will require knowledge of the bending and torsional stiffness of DNA. Meanwhile, it is important to obtain as much experimental information as possible about the molecule. In this respect, a rigorous theoretical treatment of the scattering from collections of randomly oriented helices possessing both one and two orders of coiling is necessary for proper interpretation of the diffraction patterns. Such a treatment is given in this communication. A discussion of the properties of the derived scattering curves shows that the results of Brady et al. (1976) can be interpreted in terms of a specific supercoil geometry.

METHOD AND CALCULATIONS

The intensity, in relative units, scattered per unit length from an assemblage of randomly oriented filaments of constant electron density ρ is expressed by the relation (Debye, 1915; Schmidt, 1967)

$$I(h) = \frac{\rho^2}{2} \int_0^{\mathcal{L}} d\ell_1 \int_0^{\mathcal{L}} \frac{\sin hr(p_1, p_2)}{hr(p_1, p_2)} d\ell_2, \tag{2}$$

where ℓ_1 and ℓ_2 are two copies of the length parameter, and $h = 4\pi \sin \Theta/\lambda$; λ is the wavelength of the incident radiation and Θ is one-half the scattering angle. The variable $r(p_1, p_2)$ is the distance between points p_1 and p_2 on the filament, and $\mathcal{L}$ is the length of the filament. For our purposes $\mathcal{L}$ can be conveniently taken as 1,000 Å, and ρ as unity. This equation can be integrated numerically for any filament geometry, at least in principle. We use it to treat explicitly the case of a superhelix with both one and two orders of supercoiling. This calculation applies to any helix; we use the term superhelix to indicate that the Crick-Watson double helix is not one of the orders being treated. Its scattering is in the wide angle region where the assumption of constant density is not valid.

Fig. 1 shows a first order superhelix of radius ρ_1 and axial repeat $2\pi a$; the coordinate expression is $x(\gamma) = \rho_1 \cos \gamma$, $y(\gamma) = \rho_1 \sin \gamma$, $z(\gamma) = a\gamma$. Here helices are described in terms of their pitch angle α, also shown, which is defined by the relation $\tan \alpha = \rho_1/a$.

Figs. 2 and 3 show filaments having two orders of supercoiling. The first order is superimposed on an axis which is itself a helix. A special case, the toroidal helix, is shown on Fig. 2 *a*. In this configuration the second order reduces to a circle (pitch angle = $\pi/2$). Shapes possessing two orders of helicity are referred to as coiled coils. Fig. 3 depicts the specific coiled coil treated in the text. It consists of five turns of a first order helix wound around a second order helix of pitch angle 45°. The radius ratio is $\rho_1/\rho_2 = 0.4$.

For the first order supercoil it follows from the geometry that the distance r between two

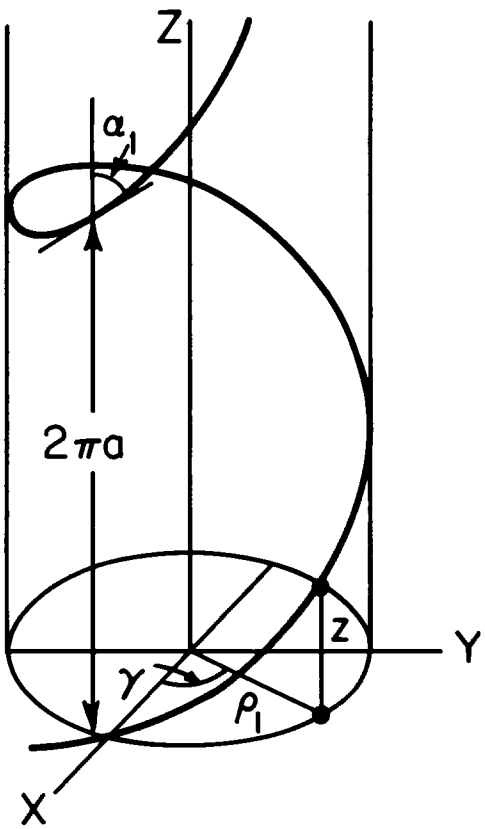

FIGURE 1 Diagram of a helix showing coordinate system, repeat distance, and pitch angle.

points $p_1 = p(\gamma_1)$ and $p_2 = p(\gamma_2)$ on the helix is given by

$$r^2(\gamma_1, \gamma_2) = 2\rho_1^2[1 - \cos(\gamma_2 - \gamma_1)] + a^2(\gamma_2 - \gamma_1)^2. \tag{3}$$

We see that r depends only on the parameter difference $\Delta\gamma = (\gamma_2 - \gamma_1) = (\ell_2 - \ell_1)/\sqrt{\rho_1^2 + a^2}$. Hence the change of variables $v = \ell_1$ and $w = \ell_2 - \ell_1$ reduces the double integral of Eq. 2 to the single integral

$$I(h) = \frac{2}{\mathcal{L}^2}\int_0^{\mathcal{L}} \frac{(\mathcal{L} - w)\sin h\psi}{h\psi}\,dw, \tag{4a}$$

where

$$\psi = +\sqrt{2\rho_1^2\left[1 - \cos\left(\frac{w}{\sqrt{\rho_1^2 + a^2}}\right)\right] + \frac{a^2w^2}{\rho_1^2 + a^2}}. \tag{4b}$$

This integral may be evaluated on a computer to any desired degree of accuracy. The results of such calculations for several helices of different pitch angles will be presented below.

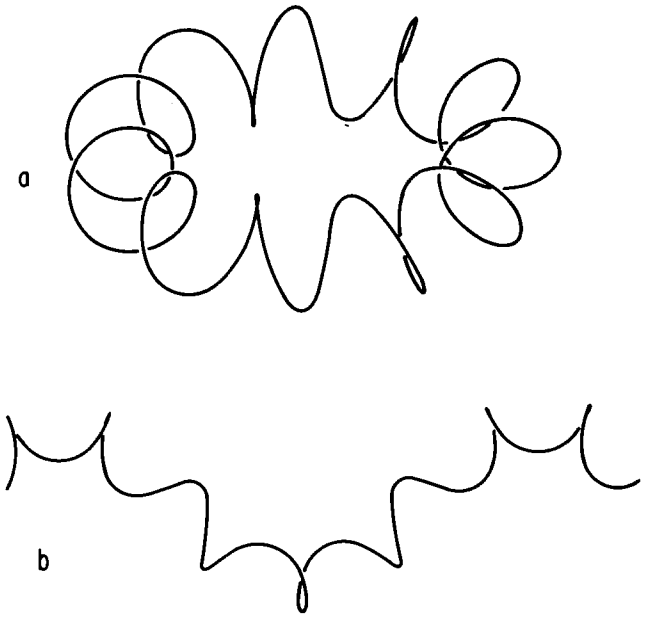

FIGURE 2 Two orders of helicity. The first order helix axis is itself a (second order) helix. If the pitch angle of the second order is $\pi/2$ a toroidal helix results (2 *a*). Combinations of two helical orders are referred to as coiled coils.

Other authors have considered the theoretical scattering from randomly oriented helices. The case of infinitely long helices was first treated by Kirste (1964) using a summation technique different from the present numerical integration. Fedorov and Aleshin (1966) determined the scattering from finite single helices by an integration method closely related to that developed here. The integral of Eq. 4 a, although derived independently, may be shown to reduce to that of Fedorov and Aleshin by a change of variables and trigonometric substitutions. Schmidt (1970) found the scattering intensity from random, infinitely thin single and double helical structures by directional averaging of the oriented intensities. Puigjaner and Subirana (1974) have evaluated the scattering from randomly oriented double helical structures of finite thickness.

For the case of coiled coils (Crick 1953) with first and second order radii ρ_1 and ρ_2, respectively, and with N first order turns for each turn of the second order, a point p is given

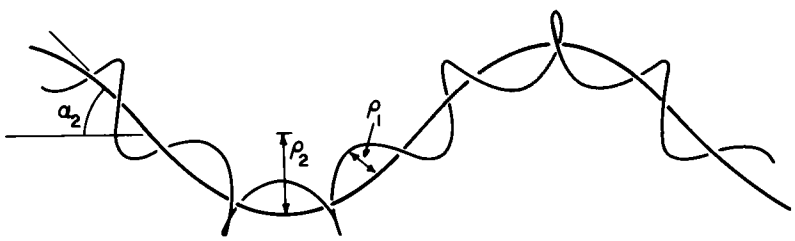

FIGURE 3 The coiled coil whose calculated scattering pattern is shown in Fig. 7. The pitch angle α_2 of the second order is 45° and the radii are in the ratio $\rho_2/\rho_1 = 0.4$. The number N of turns of the first order per second order turn is 5.

by $p(\gamma) = [x(\gamma), y(\gamma), z(\gamma)]$, where

$$x(\gamma) = \cos\gamma\,(\rho_2 + \rho_1 \cos N\gamma) - \rho_1 \cos\alpha_2 \sin\gamma \sin N\gamma \tag{5a}$$

$$y(\gamma) = \sin\gamma\,(\rho_2 + \rho_1 \cos N\gamma) + \rho_1 \cos\gamma \sin N\gamma \cos\alpha_2 \tag{5b}$$

$$z(\gamma) = a\,\gamma - \rho_1 \sin\alpha_2 \sin N\gamma. \tag{5c}$$

In this case the integral in Eq. 2 cannot be reduced in dimension by any obvious substitution. The distance $r\,(p_1, p_2)$ between the points $p_1 = p(\gamma_1)$ and $p_2 = p(\gamma_2)$ on the filament now depends explicitly on the values γ_1 and γ_2, not just on their difference $\Delta\gamma = (\gamma_2 - \gamma_1)$. More explicitly one may show that

$$d\ell = \sqrt{f(\gamma)}\,d\gamma, \tag{6a}$$

where

$$f(\gamma) = \rho_2^2 + \rho_1^2 N^2 + \rho_1^2\,(\cos^2 N\gamma + \sin^2 N\gamma \cos^2\alpha_2) + a^2 + 2\rho_2\rho_1 \cos N\gamma + 2\rho_1^2 N \cos\alpha_2. \tag{6b}$$

Also, from Eq. 5 a, b, and c

$$\begin{aligned} r^2(\gamma_1, \gamma_2) = {} & 2[\rho_2^2 + \rho_1^2 + \rho_2\rho_1\,(\cos N\gamma_2 + \cos N\gamma_1)] \\ & + a^2(\gamma_1 - \gamma_2)^2 - 2\cos(\gamma_1 - \gamma_2)[\rho_2^2 + \rho_2\rho_1\,(\cos N\gamma_1 + \cos N\gamma_2) \\ & + \rho_1^2\,(\cos N\gamma_2 \cos N\gamma_1 + \sin N\gamma_2 \sin N\gamma_1 \cos^2\alpha_2)] \\ & - 2\sin(\gamma_1 - \gamma_2)[\rho_2\rho_1 \cos\alpha_2(\sin N\gamma_2 - \sin N\gamma_1) \\ & - \rho_1^2 \cos\alpha_2 \sin(\gamma_1 - \gamma_2)] - 2\rho_1^2 \sin N\gamma_1 \sin N\gamma_2 \sin^2\alpha_2 \\ & + 2a\rho_1 \sin\alpha_2\,(\sin N\gamma_2 - \sin N\gamma_1)(\gamma_1 - \gamma_2). \end{aligned} \tag{7}$$

Using this expression for $r(\gamma_1, \gamma_2)$ and the substitutions given in Eq. 5 a,b the scattering equation for a coiled coil becomes

$$I(h) = \frac{1}{\mathcal{L}^2} \int d\gamma_2 \int \sqrt{[f(\gamma_2) f(\gamma_1)]}\,\frac{\sin hr(\gamma_1, \gamma_2)}{hr(\gamma_1, \gamma_2)}\,d\gamma_1. \tag{8}$$

The solution to this double integral is computed numerically using quadratures. Since the

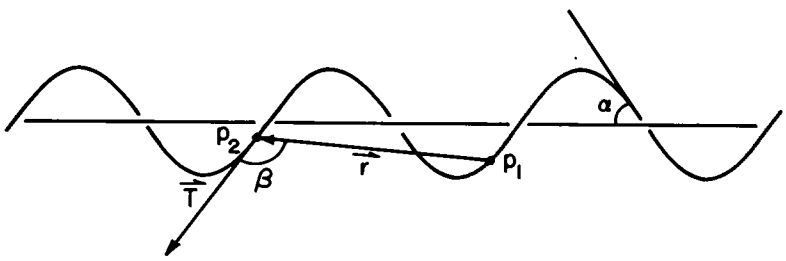

FIGURE 4 A distance vector r between points p_1 and p_2 on the helix makes an angle β with the tangent vector T to the helix at p_2. A spherical shell of radius r and thickness dr about p_1 contains maximal scattering material exactly when $|\cos\beta|$ is minimized.

accuracy of the numerical integration falls off for large h (corresponding to small distances r), the chosen grid size into which the area of integration is subdivided must be considerably smaller than the repeat distance of the first order helix. Use of a fine mesh grid increases the time necessary to perform the calculation. Thus this integral was evaluated for only the one geometry of the coiled coil shown in Fig. 3.

A treatment of the scattering from oriented discontinuous coiled coils has been given by Crick (1953). His approach is based on the Fourier transformation of the electron density distribution, in contrast to ours, which is essentially an integration over electron pairs. However his treatment could presumably be extended to the random continuous coiled coil by suitable reduction and averaging over all orientations.

RESULTS AND DISCUSSION

The Scattering Profiles

For convenience we assume a contour length of L = 1,000 Å per turn in the treatment of the helical case. For the coiled coil we choose one turn of the second order helix (the helical central axis in Fig. 3) to be 1,000 Å, and containing five turns of the first order helix. The radius of the helix varies with pitch angle as $2\pi\rho_1 = 1{,}000 \sin \alpha$. To scale to other lengths, one simply rescales h so that Lh remains constant. This follows from the Bragg equation averaged

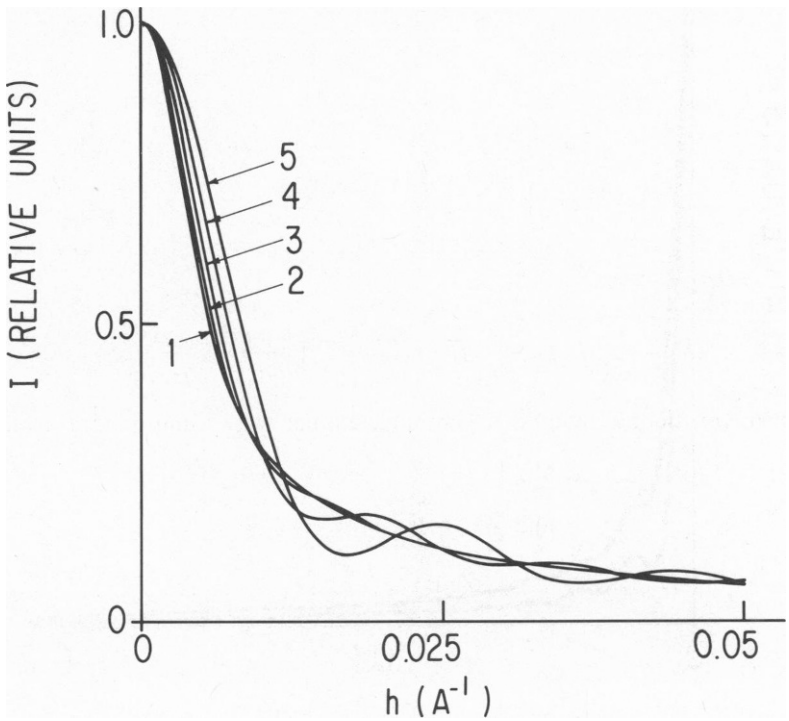

FIGURE 5 Intensity pattern of a randomly oriented filament consisting of one helical turn and different values of the pitch angle α_1. Comparison with Tables I and II shows that h for the first maximum is determined by the geometric condition of minimization of $|\cos \beta|$ (see text). *1*, α = 15°; *2*, α = 30°; *3*, α = 45°; *4*, α = 60°; *5*, α = 75°.

for random orientation (Zernicke and Prins, 1927) $\rho_1 = 1.23\ (\lambda/2 \sin \Theta) = 7.73/h$. Here each helix order is specified by its pitch angle and contour length per turn instead of the more commonly used pitch and radius. These two sets of parameters can be easily interchanged, using for example Eq. 9 and the definition $\tan \alpha = \rho/a$.

To start, we focus on the first order superhelix whose scattering is defined by Eq. 4 a,b. Plots of the scattering factors for five different values of α are shown in Fig. 5. The curves show that up to pitch angles of $\simeq 20°$ the patterns are indistinguishable from that of a rodlike filament. When $\alpha \simeq 45°$ a shoulder appears at $h = 0.015$. With further increase in pitch angle this shoulder moves out to a larger angle and changes into a well defined peak. For the largest pitch angle shown, $\alpha = 75°$, the peak maximum is centered at $h \simeq 0.024$. These curves were calculated for a filament one-turn long. Fig. 6 compares the scattering per unit length for one and two turns of a helix with $\alpha = 60°$. As the figure shows, increasing the number of turns does not give rise to new diffraction effects; the net effect is rather to enhance the magnitude of the peaks already present in the single turn pattern and to shift them slightly to smaller angles. A first conclusion from these two results is that the scattering does not depend primarily on correlations between electrons in neighboring turns, but on electron pair correlations in a single turn. In fact, an analogous analysis (using Eq. 4 a) for a helix of less

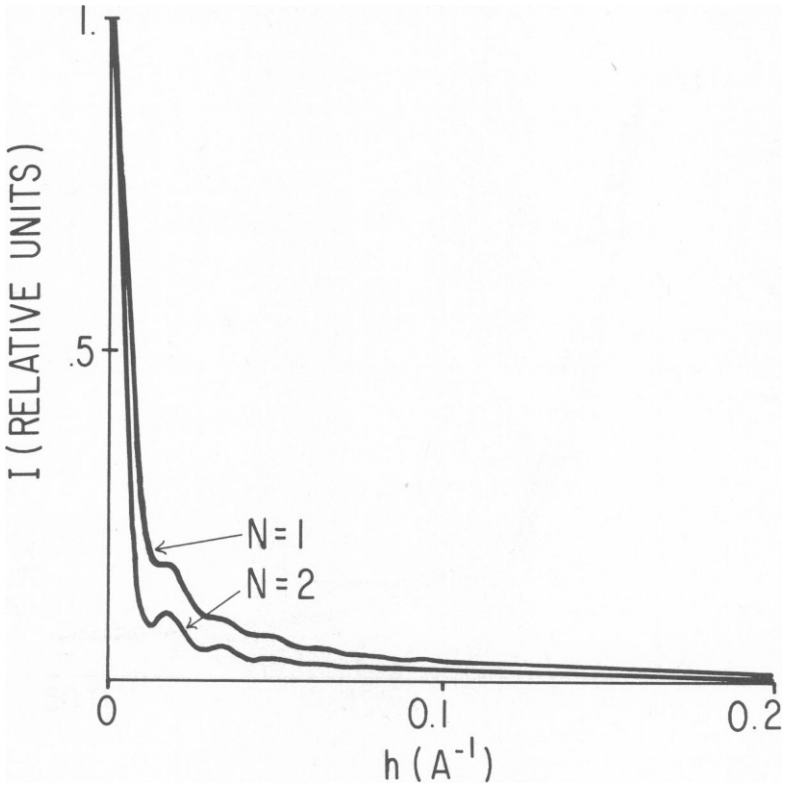

FIGURE 6 Scattered intensity/unit length for helices of pitch angle 60° and N turns. The maxima and minima are more pronounced for larger numbers of turns.

than one complete turn shows that scattering maxima are present in this case also.[1] Finally, the scattering maxima show that it is not quite correct to analyze the data in terms of a Bragg's law relation linking the observed spacing to a helix pitch or radius, as was done in the original publication (Brady et al., 1976). Taking, for example, a helix of 1,000 Å contour length and a pitch angle of 45° (curve 3, Fig. 5), we have, from the helix relation

$$L^2 = 4\pi^2 \rho_1^2 + p^2, \tag{9}$$

that $\rho_1 = a = 112.5$ Å and $p = 2\pi a = 707.1$ Å. Substituting these in the expression

$$\left(\frac{1.23}{d_{\text{Bragg}}}\right)^2 = \left(\frac{1.84}{2\pi\rho_1}\right)^2 + \left(\frac{1}{p}\right)^2, \tag{10}$$

we get a true $d_{\text{Bragg}} = 633$ Å. In actuality the maximum in curve 3 corresponds to a Bragg spacing of 415 Å, which, if inserted in Eq. 10, would give unrealistic values for the pitch and radius.

These findings are not surprising when we consider that for these randomly oriented helices the maxima in the scattering curves depend primarily on the properties of the electron pair correlation function, $C(r)$. This function, multiplied by $4\pi r^2\, dr$, gives the number of electron pairs at distances between r and $r + dr$ from any electron in the helix. In fact, Eq. 4 a can be written in terms of $C(r)$ as

$$I(h) = \frac{2}{L}\int_0^{r_{max}} C(r)\,\frac{\sin hr}{hr}\,dr \tag{11}$$

A geometrical conception of $C(r)$ is shown in Fig. 4. A shell of radius r and thickness dr is drawn about the point p_1 such that a point p_2 in the helix at distance r lies within this shell. Let **T** be the tangent vector to the helix at p_2 and **r** be the distance vector between p_1 and p_2. Finally, let β be the angle between **T** and **r**. The amount of scattering matter contained within this shell is proportional to the length $d\ell$ of the segment it contains. Clearly $d\ell = dr/|\cos\beta|$, so $d\ell$, and therefore $C(r)$ are maximal when $|\cos\beta|$ is minimized. Manipulation of the equations show that

$$\cos\beta = \frac{\rho_1^2[\sin(\gamma_2 - \gamma_1) + (\gamma_2 - \gamma_1)/\tan^2\alpha]}{\{(a^2 + \rho_1^2)[2\rho_1^2(1 - \cos(\gamma_2 - \gamma_1)) + a^2(\gamma_2 - \gamma_1)^2]\}^{1/2}}. \tag{12}$$

Like $r(\gamma_1, \gamma_2)$ in Eq. 3, $|\cos\beta|$ for a first order helix depends only on the difference $\Delta\gamma = (\gamma_2 - \gamma_1)$, and thus $C(r)$ will peak at those values of r corresponding to the $\Delta\gamma$'s which minimize cos β. The properties of cos β as they relate to the helical geometry are discussed below. For the present, we note that the positions of the peak maxima are determined by the smallest values of $\Delta\gamma$ for which $|\cos\beta|$ is minimized.

The same geometrical considerations determine the scattering from the coiled coil.

[1]This finding answers the main criticism of our model by Campbell (1977), who felt that it was incompatible with his branched structures, since the length of the branches is less than one turn of the second order helix. It is not necessary that the branches encompass at least one turn for them to exhibit the helical scattering.

However, this structure is not self-similar. That is the geometrical relationships between pairs of points depends on the specific points chosen, not just on the value of $\Delta\gamma$ between them. Thus the relationships between r, $\Delta\gamma$, and $|\cos\beta|$ are not as straightforward as in the first order helix.

The scattering curve for one repeat unit of the coiled coil, calculated from Eq. 8 for the specific geometry in Fig. 3, is displayed in Fig. 7. In this case the corresponding pitch angle and contour length of one first order turn are 55° and ~345 Å, respectively. Two features are to be noted. First there is a peak which appears as a shoulder, centered at $h = 0.015$ arising from the scattering from the second order. Since the scale of Fig. 7 has been chosen such that its second order helix has the same length as the first order helix of Fig. 5, in the absence of perturbing effects its maximum should occur at the same value of h as that curve in Fig. 5 with the same pitch angle (45°). Examination of curve 3 in that figure shows that this is indeed true, and that the second order helix curve is quite similar to that of the first order curve over a range of h extending from $h = 0$ to values of h considerably beyond $h = 0.015$. The only difference is a slight broadening of the peak, caused by the deformation due to the presence of the first order.

The second feature is the series of peaks, the first of which is centered at $h = 0.053$. This part of the profile is the first order helix scattering. Again, the pattern is quite similar to that

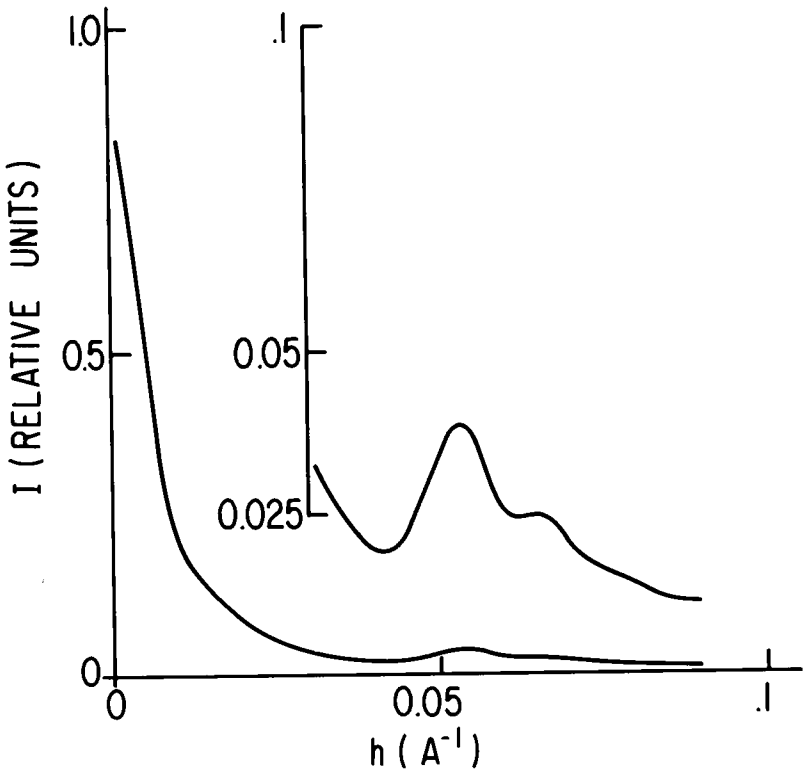

FIGURE 7 Intensity pattern of the coiled coil shown in Fig. 3. The ordinate has been amplified by a factor of 10 at $h \geq 0.03$. The maximum at $h = 0.053$ and the shoulder at $h \simeq 0.015$ arise from the first and second order, respectively.

for a pure helix. The peak maximum for the pure helix occurs at $h = 0.050$. This slight shift again is due to the deforming influence of the other order, which brings corresponding points on the average closer together. Geometrically, this deformation causes $|\cos \beta|$ to be minimized for pairs of points whose $\Delta\gamma$'s are spread over a range of values. In sum the scattering from each order is slightly broadened by the presence of the other, but their peak locations and magnitudes are not appreciably altered. (Obviously this will only hold when the length per turn of each order is sufficiently different to prevent excessive overlap of their respective scattering functions, but practically all coiled coils are of this form). This virtual independence of the scattering from each order assures that the relative position and magnitude of the first and second order peaks must be solely a function of the mechanical properties of the molecule itself. This is an important result and will have significance in future calculations of the relationship between the scattering functions and the elastic properties of DNA.

$|Cos\ \beta|$

As shown above, maximal scattering arises from distances between points on a helix at which the factor $|\cos \beta|$ is minimized. The behavior of $|\cos \beta|$ is acutely sensitive to the helix pitch angle. Indeed, the relationship in Eq. 12 is the most important determinant of the scattering profiles shown in Figs. 5, 6, and 7. More precisely, the behavior of $|\cos \beta|$ separates helices into two classes. There exists a value of $\alpha = \alpha_c$ above which values of $\Delta\gamma = \gamma_2 - \gamma_1$ exist for which $\beta = \pi/2$, so that $\cos \beta = 0$. From Eq. 12 this occurs when

$$\sin(\Delta\gamma) = -\Delta\gamma/\tan^2\alpha. \tag{13}$$

This is the value of α for which the curve $\sin \Delta\gamma$ and the line $(-\Delta\gamma/\tan^2\alpha)$ intersect at a common point of tangency with $\Delta\gamma \neq 0$. It can be shown that for there to be nonzero values of $\Delta\gamma$ satisfying Eq. 12, α must exceed a value $\alpha_c = 1.1346$ rad (65.01°). We discuss the behavior of Eq. 12 for the two cases of helices with $\alpha < \alpha_c$ and with $\alpha > \alpha_c$. We emphasize that there is no physical difference between the two types and that the distinction is a purely mathematical one.

$\alpha < \alpha_c$ For helices of pitch angle $\alpha < \alpha_c$ there are no values of $\Delta\gamma$ for which $|\cos \beta| = 0$. However there always exists a value of $\Delta\gamma$ for which $|\cos \beta|$ is minimized. With increasing α, the minimum value of $|\cos \beta|$ decreases and the corresponding peak in the scattering pattern increases in magnitude. This is shown in Table I, where the values of $|\cos \beta|$

TABLE I

$\alpha < \alpha_C$. MINIMUM VALUE OF $|\cos \beta|$ AND CORRESPONDING VALUES OF $\Delta\gamma$, r, AND h FOR VARIOUS PITCH ANGLES

α	$\Delta\gamma$	r	h	$\cos \beta$
(degrees)	*(rads)*	*(Å)*		
5	4.0870	648.46	0.01192	0.99396
15	4.0987	634.32	0.01218	0.94574
25	4.1236	606.52	0.01274	0.84983
35	4.1655	565.91	0.01366	0.70706
45	4.2311	513.61	0.01505	0.51822
55	4.3327	450.59	0.01715	0.28335
65	4.4932	376.83	0.02051	0.00033

at its minimum are listed for increasing values of α, along with the corresponding values of $\Delta\gamma$, r, and h. Comparison with Fig. 5 shows that the magnitude of cos β at the various values of h at which the peak maxima occur mirrors exactly the trend in the magnitude of the peaks in the scattering curves.

$\alpha > \alpha_c$ For these helices the scattering is determined by the number of values of $\Delta\gamma$ which make $|\cos\beta| = 0$. As the pitch angle approaches $\pi/2$ the number of such values become very large, as shown in Table II. Calculations show that there exist values of $\alpha = \alpha_i$, $i = 1$ $(= c)$, 2, 3 such that if $\alpha_i < \alpha < \alpha_i + 1$, then Eq. 12 is solved by exactly $2i$ different values of $\Delta\gamma$; if $\alpha = \alpha_i$ there are $2i-1$ such values. Table II lists the first five values of α_i along with corresponding values of $\Delta\gamma$ for which $|\cos\beta| = 0$. The large increase in the number of values of $\Delta\gamma$ is manifested in the scattering curves by the corresponding intensification of the peak maximum with increasing α.

Of course, for all these distances r to contribute to the scattering, the filament must contain a sufficient number of turns for there to be pairs of points separated by these distances. The relative contributions of the appropriate $\Delta\gamma$s will depend directly on the number of pairs of points separated by this value of $\Delta\gamma$. Hence it follows that for any pitch angle the smallest values of $\Delta\gamma$ will predominate in their contribution to the scattering, since there are more of them. Some of the larger $\Delta\gamma$s (and longer distances) will contribute very little to the scattering. As the number of turns increase pairs of points in adjacent turns will have $\Delta\gamma$s which can contribute. For this reason the scattering profile for two or more turns is not given only by the sum of the profiles for the individual turns, as shown in Fig. 6.

TABLE II

$\alpha > \alpha_C$. VALUES OF $\Delta\gamma$ FOR WHICH $|\cos\beta| = 0$

α_i	α	$\Delta\gamma$	r	h
(degrees)	*(degrees)*	*(rad)*	*(Å)*	
$\alpha_1 = 65.01$	65.01	4.4934	376.74	0.0205
	70	3.6456	351.12	0.0220
		5.4723	320.39	0.0241
$\alpha_2 = 73.19$	75	3.3872	335.53	0.0230
		5.8497	249.87	0.0309
		10.2520	507.55	0.0152
		11.5842	498.72	0.0155
$\alpha_3 = 76.46$				
$\alpha_4 = 78.35$				
$\alpha_5 = 79.62$				
	80	3.2426	325.65	0.0237
		6.0926	171.00	0.0452
		9.7322	410.25	0.0188
		12.1781	341.96	0.0226
		16.2372	541.22	0.0143
		18.2463	512.80	0.0151
		22.7781	692.90	0.0112
		24.2774	683.43	0.0113
		29.4299	854.69	0.0090
		30.1967	853.63	0.0090

The corresponding values of r and h are also listed, as well as the first five values of α_i.

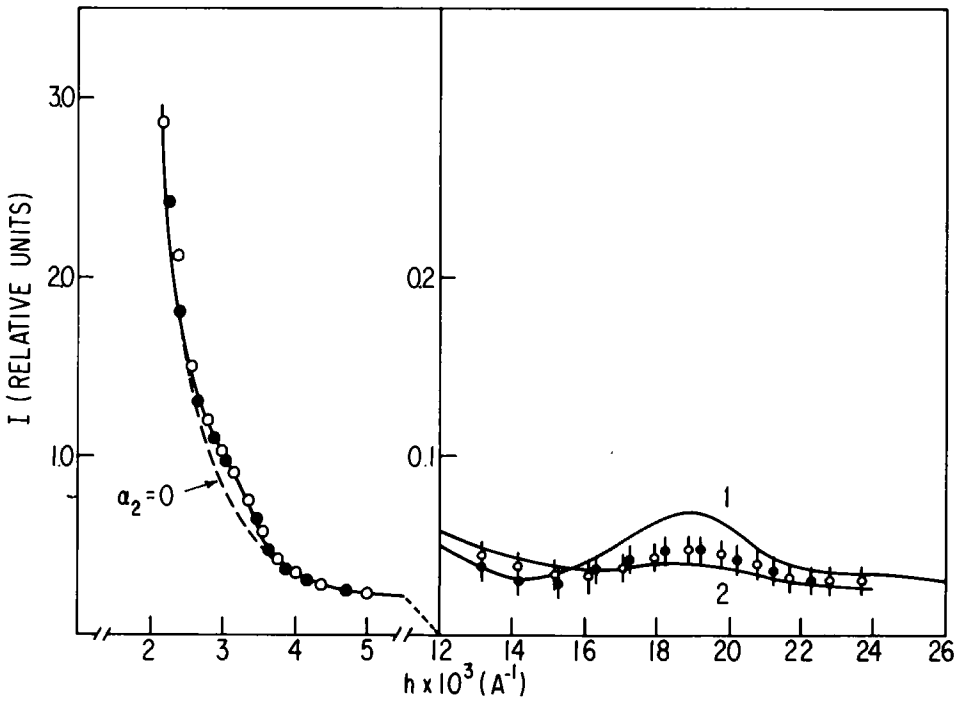

FIGURE 8 Experimental and theoretical curves. The experimental points are for samples of PM2 bacteriophage DNA (open circles) and for *E. coli* K_{12} strain C_{600} plasmid DNA (filled circles). Concentrations were 2 mg/ml. The theoretical curves are calculated for a coiled coil with second order pitch angle of 25° and first order pitch angles of 45° and 55°. The dashed line shows the shape of a first order helix curve ($\alpha_2 = 0$) in that region.

Comparison with Experiment

Experimental X-ray data on dissolved superhelical DNA is still scanty, mainly due to the low intensities involved and the susceptibility of the molecules to nicking by the X-rays. Nevertheless, sufficient data is presently available to permit comparison of theoretical and experimental curves. As shown below, the observed scattering is compatible with a coiled coil structure for superhelical DNA, the geometry of which may be estimated from the data.

Fig. 8 shows two experimentally measured scattering curves, one from PM2 viral DNA (open circles) and the other from PBR 313 plasmid DNA,[2] isolated from *Escherichia coli* K12 strain C_{600} (filled circles), into which *Pt* has been intercalated (Jennette et al., 1974) to increase the electron density contrast. The intensities determined on the first sample have been scaled up to correspond to those of the second sample. Since the inner portions of the patterns were measured with a Bonse-Hart diffractometer (Anton Paar KG, Gratz, Austria) and the outer portions with a Kratky apparatus, two instruments of completely different geometries, the construction of a composite curve is not straightforward. It was not possible to extend the measurement range of each instrument so that the data from the two overlapped. Accordingly, the curve determined at the low angles was extrapolated outward and that at the

[2]These results will be presented in detail elsewhere.

higher angles extrapolated inward until the extrapolated portions had sufficient overlap to allow normalization to the same relative intensity scale. Also shown (full lines) are two scattering curves calculated by the method described in the preceding section. The first curve is for a coiled coil with first and second order pitch angles of 55° and 25°, respectively, while the second has corresponding pitch angles of 45° and 25°. Unfortunately, the experimental data could not be desmeared due to experimental conditions (Brady et al., 1976). However, since we are interested primarily in the positions and relative shapes of the peaks in the patterns, these curves are adequate for estimating supercoil geometry.

As Fig. 8 shows, the second order portions of both experimental scattering profiles are matched quite well by the calculated curve for a helix of pitch angle 25° scaled so that its maximum lies at $h = 0.0032$. This leads to a value of ~4,900° Å for the contour length of one turn of the second order (this is the length of the helical central axis of Fig. 3, not of the coiled coil itself).

The first order portions of the experimental curves are slightly different for the two types of DNA studied. This is not surprising, as the different degrees of supercoiling and the effect of intercalating platinum into one sample may conspire to alter the DNA geometry. However, as the data have not been desmeared, it is probably inadvisable to ascribe significance to such small differences. Both sets of data lie between the calculated curves for first order helices of pitch angles 45° and 55°, respectively. The peak maximum at $h = 0.020$ corresponds to a contour length of ~920 Å/ turn. The length of the central axis of one turn of this helix is ~590 Å, so there are 8.5 turns of the first order per turn of the second.

CONCLUSIONS

It has been shown that the experimental scattering curves from supercoiled DNA are consistent with a coiled coil geometry. Theoretical considerations by Benham (1979*a*,*b*) show that highly supercoiled DNA will have denatured sites scattered around the ring, with linear segments of stressed duplex DNA lying between them. These segments assume an equilibrium structure approximating that of a coiled coil. Stable denatured regions develop when the DNA helix is underwound by 1.8% (Benham 1979*b*), so this value can be taken as the lower limit for the highly stressed configuration. (A slightly supercoiled molecule has no denatured sites so the whole ring deforms to an equilibrium shape approximating that of a toroidal helix [Fig. 2 *a*].) Native PM2 DNA is underwound by ~6% and therefore has substantial denaturation. The winding data for the plasmid PBR313 DNA are not available, but the similarity between its scattering and that of PM2 DNA indicates that it too is highly supercoiled. Therefore the experimental results are consistent with the model proposed by Benham (1977). It is wise to limit our conclusions to this statement until more experimental data is available. As noted, the experimental curves are smeared data, and in this context the agreement theory and experiment is quite satisfactory. The effect of desmearing the curves would be to sharpen the peaks, suggesting qualitatively that the true pitch angles of the DNA are somewhat greater than those deduced from the data in its present form. Also, it should be noted that the effect of internal motions of the molecule has not been taken into account. Some caution should be exercised in seeking further agreement between theory and experiment until this is done. The treatment of the influence of thermal fluctuations on the scattering profiles is a difficult problem with large molecules like superhelical DNA, and will

be given in a separate publication. For the present it should be noted that experimental evidence suggest that these motions may have relatively little net effect on the overall rigidity of the structure. It is found for example that otherwise identical DNA molecules which are supercoiled to even a slightly different degree are readily separated into discrete bands by gel electrophoresis (Keller, 1975). The sharpness of these bands, even for long molecules, suggests that the differing shapes produced by the different degrees of supercoiling are quite specific, and not at all averaged out by the fluctuations. From a theoretical view, the constraint of ring closure introduces a coupling between bending and twisting (Crick, 1976; Fuller, 1971) which greatly increases the stiffness of the molecule relative to linear DNA's. This may account for the persistence length of several thousand angstroms observed in these structures (Bloomfield et al., 1974).

A somewhat different interpretation of the X-ray data has been suggested by Subirana and Puigjaner (1977). They assert that the first order scattering is consistent with a structure in which two superhelical strands are wound into a double superhelix of ~200 Å radius and pitch of ~1,200 Å, separated by a distance of 337 Å. They propose that the lower angle shoulder in the observed profile is consistent either with another order of helicity or with the presence of large loops. Their argument relies on analogies between layer line patterns and those observed with dissolved molecules, which, as we pointed out in our discussion of the scattering curves, are dubious. In addition, their resultant scattering curves do not appear to fit the data as well as those presented here. While their suggested double superhelix is a priori possible, they do not rationalize the unfavorable entropy aspects of such an elaborate structure, nor do they explain why the attractive potential between the two strands should have a minimum at this large distance rather than at the distance of closest approach (~50 Å). The strength of the present interpretation is that it is founded on the mechanical properties of the helix itself, and is thus free of these ambiguities.

We would like to thank Leonard Lerman for his encouragement during this work.

Support from National Institutes of Health grant GM 23084 and National Science Foundation grant PCM 76-07569 is gratefully acknowledged.

Received for publication 8 January 1979 and in revised form 24 October 1979.

REFERENCES

BAUER, W., and J. VINOGRAD. 1968. The interaction of closed circular DNA with intercalative dyes. *J. Mol. Biol.* **33**:141–171.

BEERMAN, T., J. LEBOWITZ. 1973. Further analysis of the altered secondary structure of superhelical DNA. *J. Mol. Biol.* **79**:451–470.

BENHAM, C. 1977. Elastic model of supercoiling. *Proc. Natl. Acad. Sci. U.S.A.* **74**:2397–2401.

BENHAM, C. 1979*a*. An elastic model of the large-scale structure of duplex DNA. *Biopolymers.* **18**:609–623.

BENHAM, C. 1979*b*. Torsional stress and local denaturation in supercoiled DNA. *Proc. Natl. Acad. Sci. U.S.A.* **76**:3870–3874.

BLOOMFIELD, V., D. CROTHERS, and I. TINOCO. 1974. Physical chemistry of nucleic acids. Harper & Row, Inc., New York.

BRACK, C., T. BICKLE, and R. YUAN. 1975. The relation of single-stranded regions in bacteriophage PM 2 supercoiled DNA to the early melting sequences. *J. Mol. Biol.* **96**:693–702.

BRADY, G., D. FEIN, and H. BRUMBERGER. 1976. X-ray diffraction studies of circular superhelical DNA at 300–10,000 Å resolution. *Nature* (*Lond.*). **264**:231–234.

CAMPBELL, A. 1976. Conformational analysis of deoxyribonucleic acid from PM 2 bacteriophage. *Biochem J.* **155**:101–105.

CAMPBELL, A. 1977. Circular superhelical DNA. *Nature (Lond.)*. **267**:728.

CAMPBELL, A., and R. EASON. 1975. Effects of DNA primary structure on tertiary structure. *FEBS Lett.* **55**:212–215.

CHAMPOUX, J., and R. DULBECCO. 1972. An activity from mammalian cells that untwists superhelical DNA. *Proc. Natl. Acad. Sci. U.S.A.* **69**:143–146.

CRICK, F. 1953. The fourier transform of a coiled coil. *Acta Cryst.* **6**:685–689.

CRICK, F. 1976. Linking numbers and nucleosomes. *Proc. Natl. Acad. Sci. U.S.A.* **73**:2639–2643.

DEAN, W., and J. LEBOWITZ. 1971. Partial alteration of secondary structure in native superhelical DNA. *Nat. New Biol.* **231**:5–8.

DEBYE, P. 1915. Zerstreuung der Röntgenstrahlen. *Ann. Physik.* **46**:809–824.

FEDOROV, B., and V. ALESHIN. 1966. *Vysokomol. Soyed.* **8**:1506.

FULLER, F. B. 1971. The writhing number of a space curve. *Proc. Natl. Acad. Sci. U.S.A.* **68**:815–819.

FULLER, F. B. 1978. Decomposition of the linking number of a closed ribbon. *Proc. Natl. Acad. Sci. U.S.A.* **75**:3557–3561.

GELLERT, M., K. MIZUUCHI, M. O'DEA, and H. NASH. 1976. DNA gyrase: an enzyme that introduces superhelical turns into DNA. *Proc. Natl. Acad. Sci. U.S.A.* **73**:3872–3876.

GRAY, H., W. UPHOLT, and J. VINOGRAD. 1971. A buoyant method for the determination of the superhelix density of closed circular DNA. *J. Mol. Biol.* **62**:1–19.

HOLLOMAN, W., R. WIEGAND, C. HOESSLI and C. RADDING. 1975. Uptake of homologous single-stranded fragments by superhelical DNA. *Proc. Natl. Acad. Sci. U.S.A.* **72**:2394–2398.

JEANETTE, K., S. LIPPARD, G. VASSILIADES, and W. BAUER. 1974. Metallointercalation reagents. *Proc. Natl. Acad. Sci. U.S.A.* **71**:3839–3843.

KELLER, W. 1975. Determination of the number of superhelical turns in simian virus 40 DNA by gel electrophoresis. *Proc. Natl. Acad. Sci. U.S.A.* **72**:4876–4880.

KIRSTE, R. 1964. Röntgenkleinwinkelstreuung an Fadenmolekülen. *Z. Phys. Chem. (Frankfurt)*. **42**:358–366.

LAU, P., and H. GRAY. 1979. Extracellular Nucleases of Alteromonas Espejiana BAL31. *Nuc. Acids Res.* **6**:331–357.

MIZUUCHI, K., M. GELLERT, and H. NASH. 1978. Involvement of supertwisted DNA in integrative recombination of bacteriophage lambda. *J. Mol. Biol.* **121**:375–392.

PUIGJANER, L., and J. SUBIRANA. 1974. Low-angle X-ray scattering by disordered and partially ordered helical systems. *J. Appl. Cryst.* **7**:169–173.

SCHMIDT, P. W. 1967. The small-angle X-ray scattering from filaments. *In* Small-Angle X-ray Scattering. H. Brumberger, editor. Gordon & Breach, New York. 17–31.

SCHMIDT, P. W. 1970. Small-angle X-ray scattering from helical filaments. *J. Appl. Cryst.* **3**:257–264.

SUBIRANA, J., and L. PUIGJANER. 1977. Circular superhelical DNA. *Nature (Lond.)*. **267**:727.

UPHOLT, W., H. GRAY, and J. VINOGRAD. 1971. Sedimentation velocity behavior of closed circular SV40 DNA as a function of superhelix density, ionic strength, counterion and temperature. *J. Mol. Biol.* **61**:21–38.

WANG, J. 1974. Interactions between twisted DNAs and enzymes. *J. Mol. Biol.* **87**:797–816.

WATSON, J., and F. CRICK. 1953. A structure for deoxyribose nucleic acid. *Nature (Lond.)*. **171**:737–738.

ZERNICKE, F., and J. PRINS. 1927. Die Beugung von Röntgenstrahlen in Flüssigkeiten als Effekt der Molekülanordnung. *Z. Physik.* **41**:184–194.